CHAPTER 27

MODEL STUDIES OF IMPULSIVELY-GENERATED WATER WAVES

Jan M. Jordaan, Jr.
Associate Professor, Department of Civil Engineering,
University of Hawaii, Honolulu, Hawaii; formerly
Research Engineer, Hydraulics, U. S. Naval Civil
Engineering Laboratory, Port Hueneme, California

ABSTRACT

The wave action due to a sudden impulse in a body of water was studied in a wave basin with beach in the laboratory. Waves were impulsively generated in the 90 ft. tank of water, 3 ft. deep, by the impact or sudden withdrawal of a paraboloidal plunger 14 ft. in diameter. The waves had a dominant height of 2 inches and period of 3 seconds, respectively, at a distance of 50 ft. from the plunger.

Such waves are scale representations of those generated by sudden impulses in the ocean, such as an underwater nuclear explosion, a sudden change in the ocean bed due to earthquakes, or the impact of a land slide. The waves produced by a downward impulse, or by an underwater explosion, form a dispersive system: whose properties are not constant as in a uniform progressive wave train. Wave periodicities, celerities and wave lengths increase with time of travel and wave heights decrease with travel distance. Theory has already been developed to predict the wave properties at a given travel time and distance for given source energy, displacement and travel path depth profile (Jordaan 1965). Measurements agree fairly well with predictions.

FACILITY

The overall dimensions of the wave basin are 94 ft. by 92 ft. by 3 ft. deep, with a 2.5 ft. water depth. The side where the plunger is located is vertical and dissipative beaches of sand on a 1:5 slope, with wave absorbers, form the side boundaries of the basin. The fourth side, opposite the plunger, consists of a test beach of sand formed to a uniform slope, 1:13.6. The toe of this beach is 48 feet, and the shoreline 82 feet away from the center of symmetry of the plunger. The wave generator plunger (wedge type) is semi-circular in plan and parabolic in section. A pneumatic piston, controlled by double-acting solenoid valving, is remote-operated to force the plunger into or out of the water in the basin.

Wave systems were generated by a single up-stroke, down-stroke, or various combinations of these in sequence. The semi-paraboloid shape of the plunger was chosen as simulating the cavity produced momentarily after an underwater explosion. Smaller paraboloidal and spherical plungers were also used for comparative tests. One available test result with an actual explosion (dynamite cap) in the wave basin was also used for comparison.

DATA OBTAINED

Records of wave motion (water surface oscillations) were made using conductivity-type sensors at various distances from the source. From these the wave properties were graphically obtained. Correlated measurements were made of the incident wave system, the deformed waves at the shore, and the induced run-up on the slope.

SCALING LAWS FOR SIMULATION OF WAVES DUE TO AN UNDERWATER EXPLOSION

Appropriate scaling laws are here given (according to Penney) by which experimental data may be used to predict prototype behavior, assuming that the similitude can be extended from chemical to nuclear explosion.

1. FORMAL DERIVATION:

The energy of an underwater (chemical) explosion is known to be about 40% converted into the pulsating bubble (Penney) which in turn converts little or most of it into the generation of waves, depending on the depth of explosion. The greatest waves will occur from a given weight of explosive charge when h, the detonation depth is roughly equal to the critical depth D, given in Table 1. The critical depth D is taken as equal to the explosion bubble radius at maximum A_m and is found from Equation (1) below.

The maximum work done in displacing the water at the time of bubble maximum thus equals 0.4E where E is the equivalent chemical energy of the explosion. (The remainder goes into shock wave and thermal radiation, both irreversible processes with neglible wave generating effect.) Assume that the maximum waves are generated when the work done at maximum bubble size is converted entirely into wave energy. Taking $h = D = A_m$ and z as the barometric water head, hence:

$$\frac{4\pi h^3 \rho g\ (h + z)}{3} = 0.4E = \text{Maximum available wave energy} \qquad (1)$$

The scaling laws permit scaling the data from one event—be it experimental, observed or theoretically computed—to another by dimensional relationships related only to the charge weight ratios and critical explosion depth.

It is customary to express the "charge diameter ratio" as $n = (W_r)^{1/3}$. In an above-water explosion the similitude law is $L_r = n$. However, this is not the case in underwater explosion as the hydrostatic pressure is scaled, whereas the air pressure is not.

From Equation (1), the energy ratio E_r being equal to W_r, the charge ratio, there results:

$$\frac{E_2}{E_1} = n^3 = \left(\frac{h_2}{h_1}\right)^3 \left(\frac{h_2 + z}{h_1 + z}\right) \quad \text{(Where z is the head of water equal to 1 atmosphere = 34')} \qquad (2)$$

hence $\frac{h_2}{h_1}$ or L_r, can no longer be equal to n for the underwater blast.

The quantity $\frac{h_2}{h_1}$ is the new scale ratio specifically valid for underwater explosions and is denoted by m since h_2 and h_1 are taken as D_2 and D_1 from Table 1. Equation 2 can be solved for given values of W_2, W_1 and hence m and n can be determined. The distinction between above water and underwater explosion scaling is important.

A. Similitude in an above-water explosion follows the scaling law: $n = (L_r, T_r^2)$ for all linear and temporal dimensions except wave height which scales as

$$n = \xi_r^2, \text{ i.e. } \xi(nx, \sqrt{n}t) = \sqrt{n}\ \xi(x,t) \tag{3}$$

and the celerity is proportional to $\sqrt{n}$

B. Similitude in an underwater explosion follows the scaling law:

$m = (L_r, T_r^2)$ including wave height.

In other words $\xi(mx, \sqrt{m}\,t) = m\,\xi(x,t)$ (4)
and the celerity is proportional to $\sqrt{m}$

Two simplifying cases may be considered:

(a) If a small scale test in a laboratory is compared with a larger scale test in nature so that $h_1 \ll Z \ll h_2$ then

$$m = n^{3/4}\left(\frac{Z}{h_1}\right)^{1/4}, \text{ or } m = W_r^{\;1/4} = \text{const.} \tag{5}$$

(b) In case of two small-scale laboratory experiments $h_1,\ h_2 \ll Z$ then $m \cong n.$ (6)

By these scaling relationships experimental data are applicable to prototype situations. The wave histories of two geometrically similar but unequal yield underwater explosions will be similar provided they are compared at homologous points in time and space. For exact geometric similitude it has been shown that the linear scale ratio m between the prototype and a scale model is proportional to $W_r^{1/4}$ where W_r is the ratio of the yields of the two cases. Here m is not only a measure of the scale ratio of the wave system emanating, but also of the explosion itself, e.g. bubble maximum diameter, and explosion crater diameter momentarily formed after the bubble breaks the water surface. Hence, for geometric similitude, the depth of detonation, basin depth and lateral dimensions must be in this ratio m as well. The wave histories are to be compared always at two homologous points whose ranges from the source's surface zero are also in this ratio m. The wave heights will for two such homologous points be related by the ratio m and the wave periods and arrival times by the ratio $\sqrt{m}$, as will be also be the group velocities and phase celerities. ($\sqrt{m}$)

The above approximation $m = W_r^{1/4}$ is valid only for the underwater explosion comparison between two unequal large scale explosions. The exact equation is $m = \frac{h_2}{h_1}$ where h_2, h_1 is found from Equation (1) above or Table 1 and will satisfy the relationship:

$$\left(\frac{h_2}{h_1}\right)^3 \left(\frac{h_2 + z}{h_1 + z}\right) = W_r \tag{7}$$

(Equation (7) is applicable only to the underwater explosion case. On the contrary in surface blasts and air blasts the scale ratio is a slightly differing quantity,

$n = (W_r)^{1/3}$, the charge diameter ratio.)

In comparing the behavior at homologous points in a scaled large yield explosion, with respect to shock wave phenomena, e.g. air and water shock, their distances from the source are generally related by the scale ratio of charge diameters, $n = W_r^{1/3}$.

The wave motions in an underwater explosion, however, are expressed in terms of the yield by the scale ratio of the bubble diameters

$m = (W_r)^{1/4}$

Glasstone's method is to calculate, "the wave height at R for a W kiloton explosion in depth y as equal to $W^{\frac{1}{2}}$ times the wave height at R for a 1 kiloton explosion at depth $\frac{y}{W^{1/4}}$." The latter quantity is known as the scaled depth. This leads to the same result as the method here given which is more exact: "the wave height at R for a W kiloton explosion in depth y is equal to $W^{1/4}$ times the wave height at $R/W^{1/4}$ for a 1 kiloton explosion at depth $y/W^{1/4}$."

THE LIMITING DEPTHS.

For a given yield exploded underwater at a depth less than the lesser limiting depth, shallow water waves will be generated. For such a case the leading wave remains the largest and is practically non-dispersive, is given by the relationship: (Glasstone)

$$Y_1 \leqq 85\ W^{1/4} \tag{8}$$

where W is the yield expressed in kilotons of TNT equivalent.

The "greater limiting depth" for larger than which an underwater nuclear explosion of a given yield will generate what is known as "deep water waves," in which the leading waves become exceedingly low and "very" dispersive, as given by the relationship

$$Y^1 = 400\ W^{1/4} \tag{9}$$

The depth, h, of the detonation point is assumed to be in all cases that which would result in the largest waves, i.e. the critical depth, which for the "shallow water wave" case is h = y/2 or mid-depth, and for the "deep water wave" case is $h = A_m$, the radius of the explosion bubble at maximum, also obtainable from Equation (1).

According to Glasstone, for explosions in depths shallower than the "lesser limiting depth" the dominant wave height will be reduced in proportion to the depth. For depths deeper than the "greater limiting depth" the dominant wave height remains unchanged from the wave height at that depth.

TABLE 1

Wave Heights for Nuclear Explosion at Mid-Depth;
for Shallow Water vs. Deep Water

			Shallow Water Explosion		Deep Water Explosion	
Yield W (In Kilo-tons)	Selected range ** R ($0.5W^{1/3}$ miles)	Scale ratio of 1 lb. model m	Water Depth* y_s (feet) Maximum for shallow water case	Wave height at given range R H_s (feet***)	Min. Depth for deep water case y_d (feet)	Wave height at given range R H_d (feet***)
1 KT	0.50	62.5	85	6.0	400	18.0
20 KT	1.35	133	180	11.2	850	33.5
200 KT	2.92	235	319	19.0	1500	49.0
2,000 KT	6.30	420	569	31.3	2680	71.5
20,000 KT	13.60	740	1010	49.5	4770	99.0

* For depths less than given in this column, height of waves will be reduced proportionally.

** For other ranges than selected range given in this column, height of waves will vary in inverse proportion, for both H_s and H_d.

*** A constant depth y_s or y_d is assumed up to the range R for which the wave heights are given. Shoaling effects thereafter may increase the heights again.

Based on scaling of Bikini Baker shot, 20 KT at mid-depth in 180' water (Glasstone).

Experimental and theoretical results Figures 2, 3 show that the period of the dominant wave (i.e. highest) in the group is relatively insensitive to the influence of depth, whether it be the "shallow water wave" or a "deep water wave" case. Moreover it is insensitive to range or distance of travel and remains a constant throughout the wave dispersion, being associated in turn with the maximum of a continually moving progression of waves in the deep water case, and with the first or one of the first waves in the shallow water case. This dominant period of the group is found by experiment to be solely a function of the dimension of the wave generating explosion bubble or crater, and hence also of the yield as indicated in Figure 16.

Examples:

1. Let the model be a simulated 1 lb. charge of TNT and the prototype a 20 Kiloton underwater NE explosion

Model charge $W_m = \frac{1}{2000\text{x}1000}$ Kilotons

Prototype charge W_p = 20 Kilotons

Bubble diam ratio $m \cong \left(\frac{W_p}{W_m}\right)^{\frac{1}{4}} \left(\frac{Z}{h_m}\right)^{\frac{1}{4}}$ from Eq (5)

$\cong 79.5 \times 1.68 \cong 133$, $(\frac{Z}{h_m} = \frac{34}{4.2})$

or from Table 1, $m = \frac{D_p}{D_m} = \frac{537}{4.2} = 128$

hence, from Equation (4), the wave height ξ of prototype is:

$\xi_p = 133 \xi_m$, where ξ_p is measured at

$$\begin{cases} \text{a range: } x_p = 133\, x_m \text{, and at} \\ \text{a time: } t_p = 11.5\, t_m \end{cases}$$

2. Use the data for the 1 lb. simulated explosion on figure 9 to scale to the prototype = 20 Kiloton UW NE explosion:

W_p = prototype yield in Kilotons = 20

$W_p^{\frac{1}{4}} = 2.115$ and $W_p^{1/8} = 1.455$

$H_p = 62.5\, W_p^{\frac{1}{4}} H_m$

$= 62.5 \times 2.115\, H_m = 133\, H_m$

at $t_p = 7.9 \times 1\ 455\, t_m = 11.5\, t_m$

at $R_p = 62.5 \times 2.115\ R_m = 133\ R_m$

3. Let the model be a simulated 1/4 lb. charge of TNT and the prototype be a 10,000 lb. HE explosion

Model Charge $W_m = \frac{1}{4x2000x1000}$ Kilotons

Prototype Charge $W_p = \frac{5}{1000}$ Kilotons

Bubble diam ratio

$$m = \left(\frac{W_p}{W_m}\right)^{\frac{1}{4}} \times \left(\frac{Z}{h_m}\right)^{\frac{1}{4}} \quad \text{from Eq 5}$$

$$= 14.2 \times \left(\frac{34}{2.45}\right)^{\frac{1}{4}}$$

$$= 14.2 \times 1.93 = 27.5$$

or from plot of Table 4 $\quad m = \frac{hp}{h_m} = \frac{70.2}{2.45} = 28.7$

Since $Z = 34'$ is comparable to both $h_m = 2.45'$ and $h_p = 85'$, Eq 5 which assumes $h \ll Z \ll h_p$ yields an inaccurate result.[p] Hence the exact equation (7) should be used.

Table 3. Height and Period of Dominant Waves

20 KT UW Nuclear Explosion

Range (ft)	Wave height (ft.) Predicted (1)	(2)	(3)	Actual (4)	Wave period (sec) Predicted only (1)	(2)	(3)
2500	39	77	41	41	23	24	21
4800	16	45	25	20	--	30	24
8000	11	26	14	13	--	34	30

(1) Glasstone p 95

(2) by Kranzer & Keller Theory, NCEL R-330 pp 58,60

(3) scaled from NCEL test, 2.0 ft withdrawal of 5.7' rad. paraboloid in 0.4 sec.

(4) Bikini BAKER, 20 KT at mid depth in 180 ft. water

Table 2 Wave-predictions for Various Yields of Shallow-Water* Underwater Nuclear Explosions

Yield	Bubble Am	At Range 8.8 Am	Height H (ft) (2)	(3)	Period (2)	sec (3)	Scale m
1 Lb.	4.07 ft.	36 ft.	34	.18	2.52	2.1	1
2 Ton	46.5	412	3.85	2.12	8.5	7.1	13.2
2 Kiloton	285	2,520	23.6	12.6	21.0	17.6	74
20 Kiloton	587	5,000	44.5	24.0	29.0	24.2	133
2 Megaton	1720	15,200	142	76	51.6	43.2	420

*Leading waves highest

(2) by Kranzer-Keller Theory

(3) by NCEL experiment, scaled up.

The annexed table from Penney 1946 gives the maximum radius of explosion bubble, A_m, versus explosive charge weight B, (TNT).

B	Am (ft.)
1 oz.	1.56
4 oz.	2.45
1 lb.	4.20
4 lb.	5.96
64 lb.	14.1
300 lb.	22.4
1000 lb.	31.4
2 Ton	46.5
2000 Ton	285

SCALING TO PROTOTYPE CONDITIONS

WAVE MOTION

Predictions were made from the observed wave motions in the laboratory of wave properties and effects in the full scale. The simulated impulsive source and its wave making effects were scaled up by the scaling laws developed by Penney, Glasstone, and others. Thus fair predictions are obtainable of wave envelope and wave properties at a point on the shore for a given source-magnitude at a given depth profile. The recorded experimental data were compared with the results from theoretical analyses of the same problem (Kranzer and Keller) as well as with limited data available from actual full-scale explosions under water (Van Dorn, Glasstone).

RUNUP

It was found that the wave run-up on the slope may be either non-breaking (as with the initial surge-wave produced by a downward plunge) or breaking (as follows immediately after the initial draw-down produced by a sudden withdrawal). In the non-breaking surge the effect is inundation, and in the breaking run-up the high velocity bore acts like a shock front on exposed structures.

The shoreline wave-height may be considerably amplified over deep water wave height as a result of refraction and shoaling by the uniform beach-slope. In these experiments the run-up height was found to be some 2½ times the shoreline wave height.

EXPERIMENTAL RESULTS

1. Water level fluctuations measured in the laboratory, when scaled to prototype according to theoretically derived scaling parameters, were found to predict the prototype water waves rather well.

2. The bubble diameter scaling relationship (Penney) was found valid for scaling laboratory measurements to prototype underwater nuclear explosions.

3. Simulated 1 lb. explosion waves in laboratory, predicted according to above, scale the waves from a 20 kt NE explosion at mid-depth in 200 feet (BAKER) Operation Crossroads, but are about 0.6 times those predicted by theory (Kranzer and Keller) for the given plunger dimensions.

4. The wave motion as distinct from the bubble motion, follows the Froude scaling law ($V_r^2 = L_r$).

5. Simulated 1/16 lb. explosion waves in laboratory predict to reasonable accuracy the waves measured in ocean due to 10,000 lb. HE explosion near the surface in 300 ft. water. Comparison with theoretical predictions (Kranzer and Keller, and Penney) is also good for this case.

6. Simulated explosion waves are found to be less dispersive when the plunger or disturbance is large relative to the water depth.

7. Waves generated by the sudden drop of a small paraboloid (diameter less than water depth) have similar dispersive properties to those of waves generated by the detonation underwater of a small dynamite cap. (Tudor NCEL TN 668.)

8. The height attenuation of waves generated in the basin by the regular plunger agreed well with that of theory by Kranzer and Keller being inversely proportional with distance. The same relationship was obtained for the waves generated by smaller dropped objects and by the small explosion.

9. Plunger motions greatly influence type of breaking and run-up, and are considered representative of various types of explosions with greatly varying breaker and run-up effects.

10. Sequencing of plunger motion through several strokes produces even larger waves of increasing steepness with number of plunges. The run-up is less than that of a single up or down stroke, however, because of dissipation by the breakers against the backwash.

FINDINGS

The principal findings are:

1. The disturbance-diameter ratio scaling relationship (Penney) was found valid for scaling wave basin measurements to prototype conditions for the simulated underwater explosions.

2. Simulated impulsively-generated waves in the laboratory are about 0.6 the height predicted by theory (Kranzer and Keller) for the same paraboloid dimensions. In the laboratory the paraboloid is suddenly withdrawn, whereas in the theory the crater is assumed to collapse naturally.

   The quick withdrawal generates waves simulating those generated by a collapse of the crater formed momentarily after the bubble escapes from an underwater explosion at depth of one bubble radius in water of depth greater than one bubble diameter.

3. The leading water surface fluctuation (a rise or a fall) depends on the geometry and phase of the disturbance. In deep water it is small to undetectable, but in shallow water displacement it is likely to be a positive crest followed by a long train of dispersive waves of ever-decreasing period, wave length and celerity. The behavior of periodicities and group envelopes experimentally obtained agree substantially with analytical theory (Kranzer and Keller).

4. The breaking and run-up of these waves are found to be related to the phase and sign as well as to the wave height and period of the individual water level fluctuations in the wave train.

The simulation of breaking and run-up of individual waves is not necessarily achieved with respect to the various possible types of disturbance.

5. Waves generated by the sudden drop of a small paraboloid (diameter less than water depth) have similar dispersive properties to those of waves generated by a deep-water explosion the underwater detonation of a dynamite cap. (Test by Tudor NCEL TN 668.)

6. In all cases the early attenuation of the wave maximum was inversely proportional to radial distance of travel, as predicted by theory (Kranzer and Keller, Penney, Lamb).

7. The speed, period and phasing of the plunger motions greatly influence the type of breaking and run-up of the leading waves.

CONCLUSIONS

The laboratory facility adequately generates dispersive wave systems by means of a sudden plunger retraction which are found to adequately simulate theoretically-predicted impulsively-generated waves.

REFERENCES

Lamb, Sir H. (1932). "Hydrodynamics" Sixth Ed. (1945), Dover Publications, New York, pp. 384-394, 429-433.

Penney, W. G. (1945), "Gravity waves produced by surface and underwater explosions." Underwater Explosion Research: V.2. The Gas Globe, U.S. Office of Naval Research, Washington, D. C., 1950, pp. 679-693.

Kranzer, H. C. and J. B. Keller (1959). "Water waves produced by explosions," Journal of Applied Physics, V. 30, No. 3, pp 398-407.

Van Dorn, W. G. (1961). "Some characteristics of surface gravity waves in the sea produced by nuclear explosions." J. of Geophys. Res. V. 66, no. 11, pp. 3845-3862.

Glasstone, S. "The effects of nuclear weapons." Rev. Edition Feb. 1964, pp. 305, 310, 311, U.S. Atomic Energy Commission, Washington 25, D. C.

Jordaan, J. M., "Run-up by Impulsively-Generated Water Waves," R-330, U.S. Naval Civil Engineering Laboratory, Port Hueneme, California, 1964.

Tudor, W. J. Uplift Pressures under a Pier Deck from Water Waves, TN 668, U. S. Naval Civil Engineering Laboratory, Port Hueneme, California, 1965.

Jordaan, J. M., "Water waves generated by underwater explosions." Paper presented at the A.S.C.E. Specialty Conference on Coastal Engineering, Santa Barbara, California, October 1965, Chapter 5 pp. 69-85 Pub. ASCE, N Y.

Jordaan, J. M., Laboratory Simulation of Waves generated by underwater nuclear explosions, T. R. No. R-424, U. S. Naval Civil Engineering Laboratory, Port Hueneme, California, 1966.

ACKNOWLEDGMENTS

The work herein reported was part of a program of research carried out at the U. S. Naval Civil Engineering Laboratory, Port Hueneme, California; and this research was supported by the Defense Atomic Support Agency of the Department of Defense. Approval for publication of this paper is gratefully acknowledged.

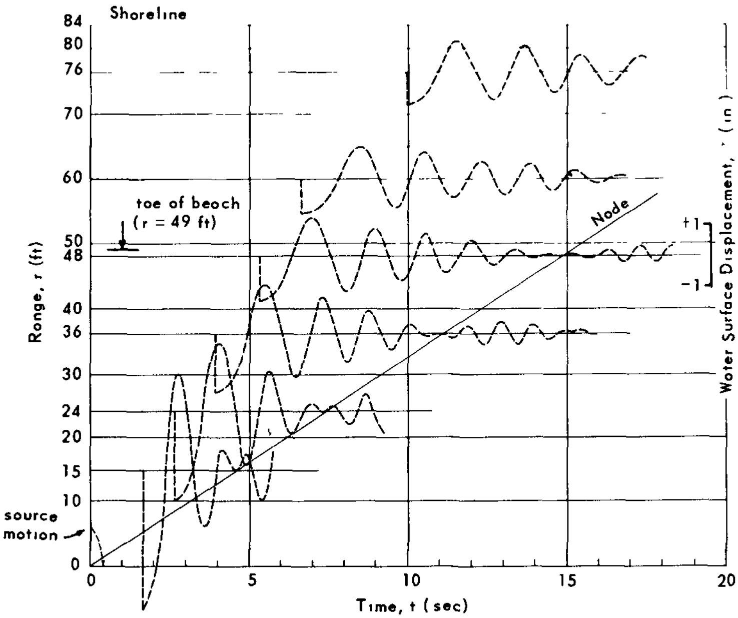

(a) Wave histories

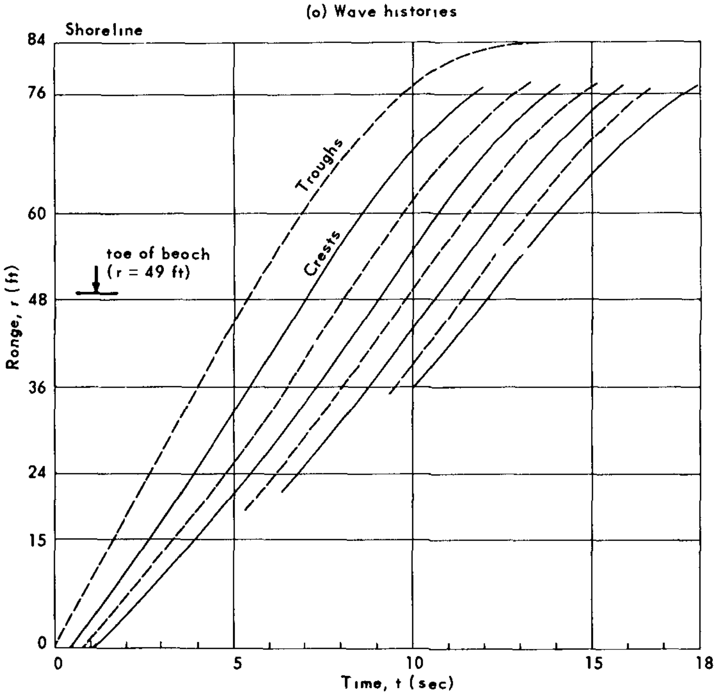

(b) Propagation characteristics

Figure 1. Theoretical wave motion for a shallow-water case: Kranzer-Keller theory for depth, d = 2.5 feet, crater radius, a = 5.7 feet (paraboloidal crater).

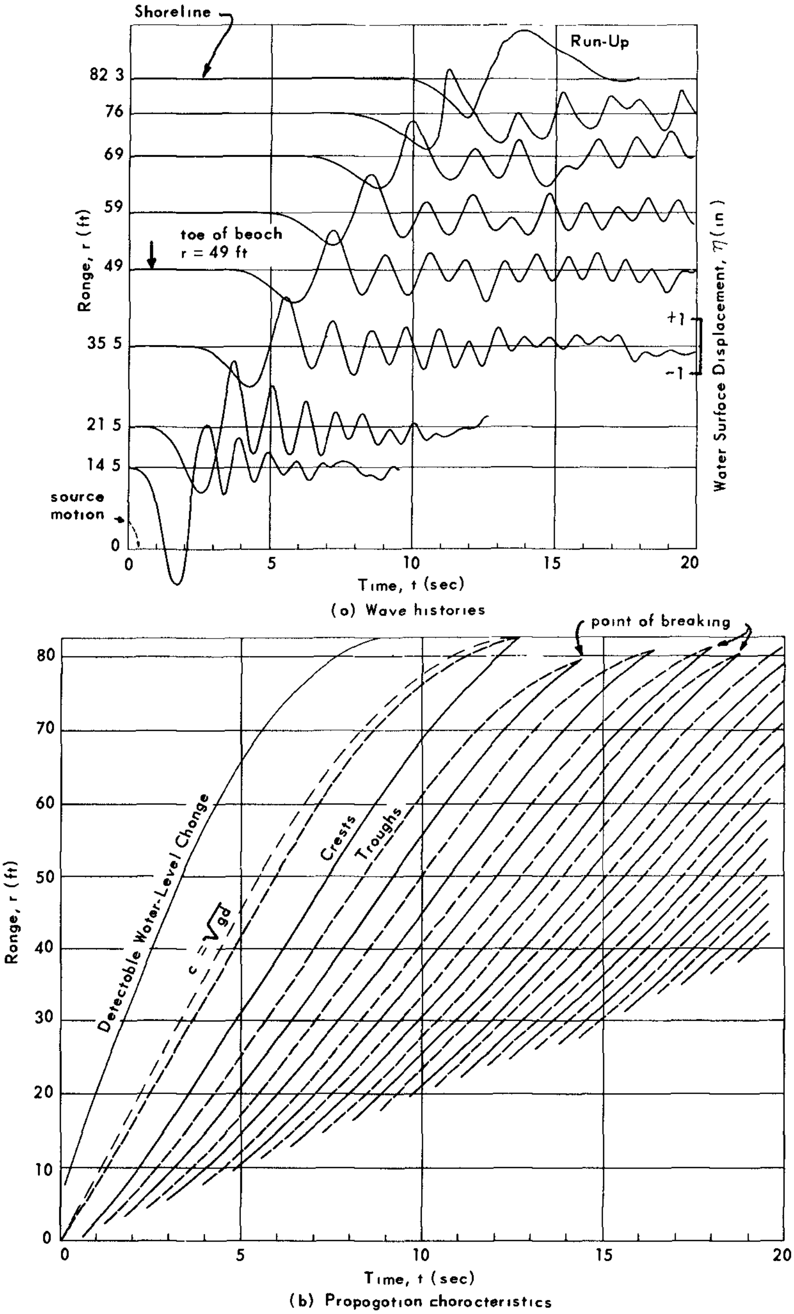

Figure 2. Experimental wave motion for a shallow-water case: NCEL data for depth, d = 2.5 feet, crater radius, a = 6.4 feet (large plunger).

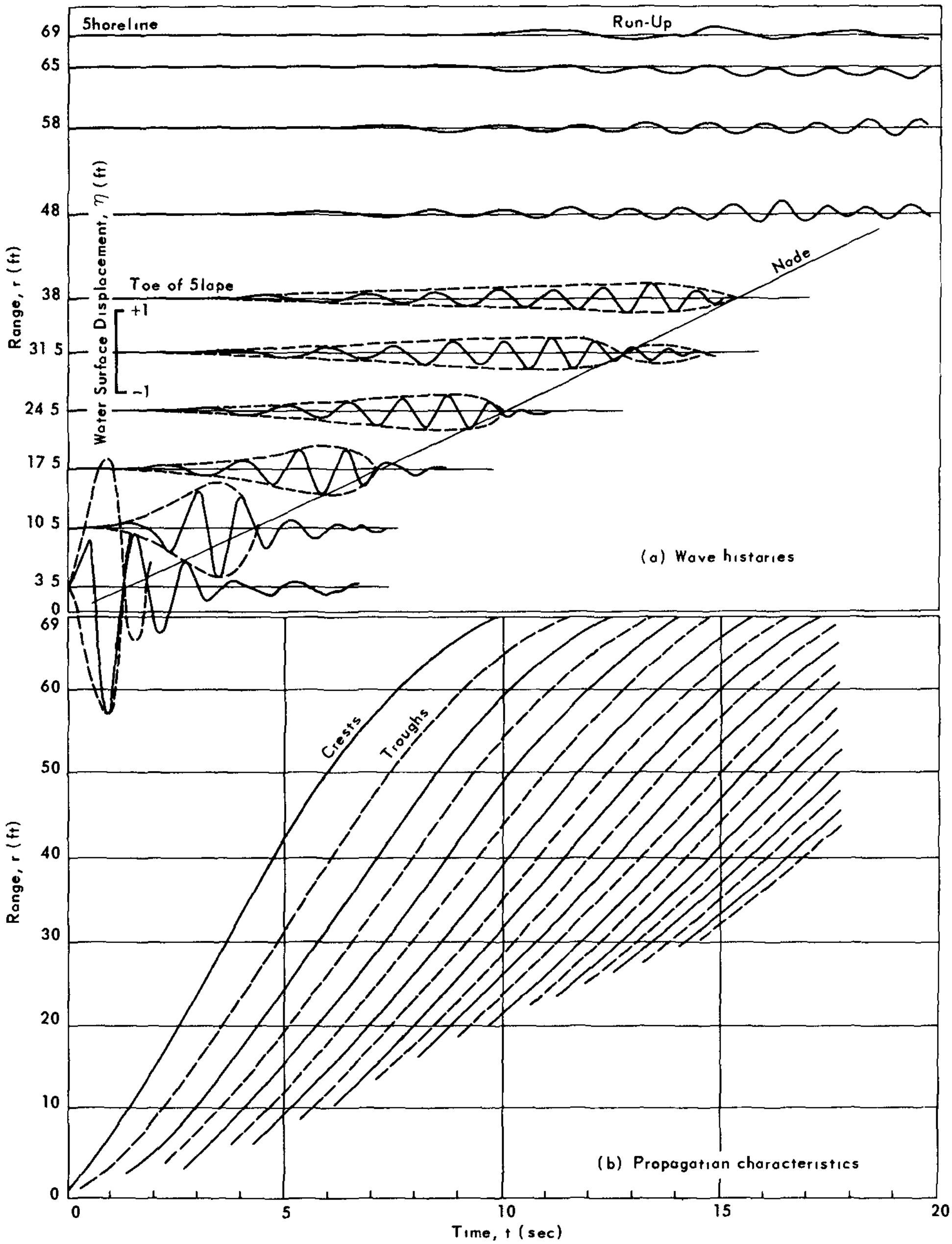

Figure 3. Experimental wave matian far an intermediate-depth case: NCEL data far depth, d = 2.5 feet, crater radius, a, approximately 3 feet (spherical buoy).

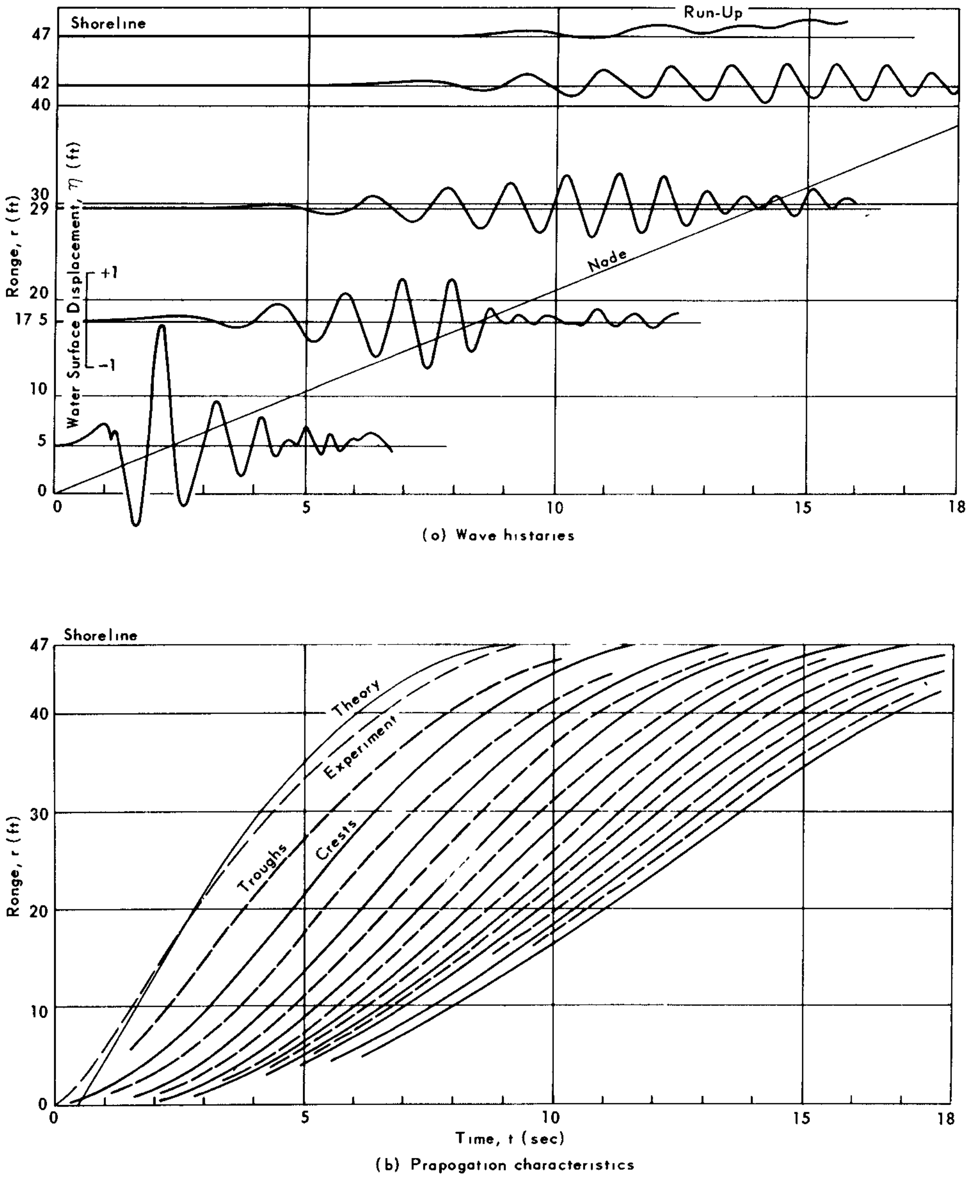

Figure 4. Experimental wave motion for a deep-water case: NCEL data for depth, d = 2.5 feet, crater radius, a, approximately 2 feet (small plunger).

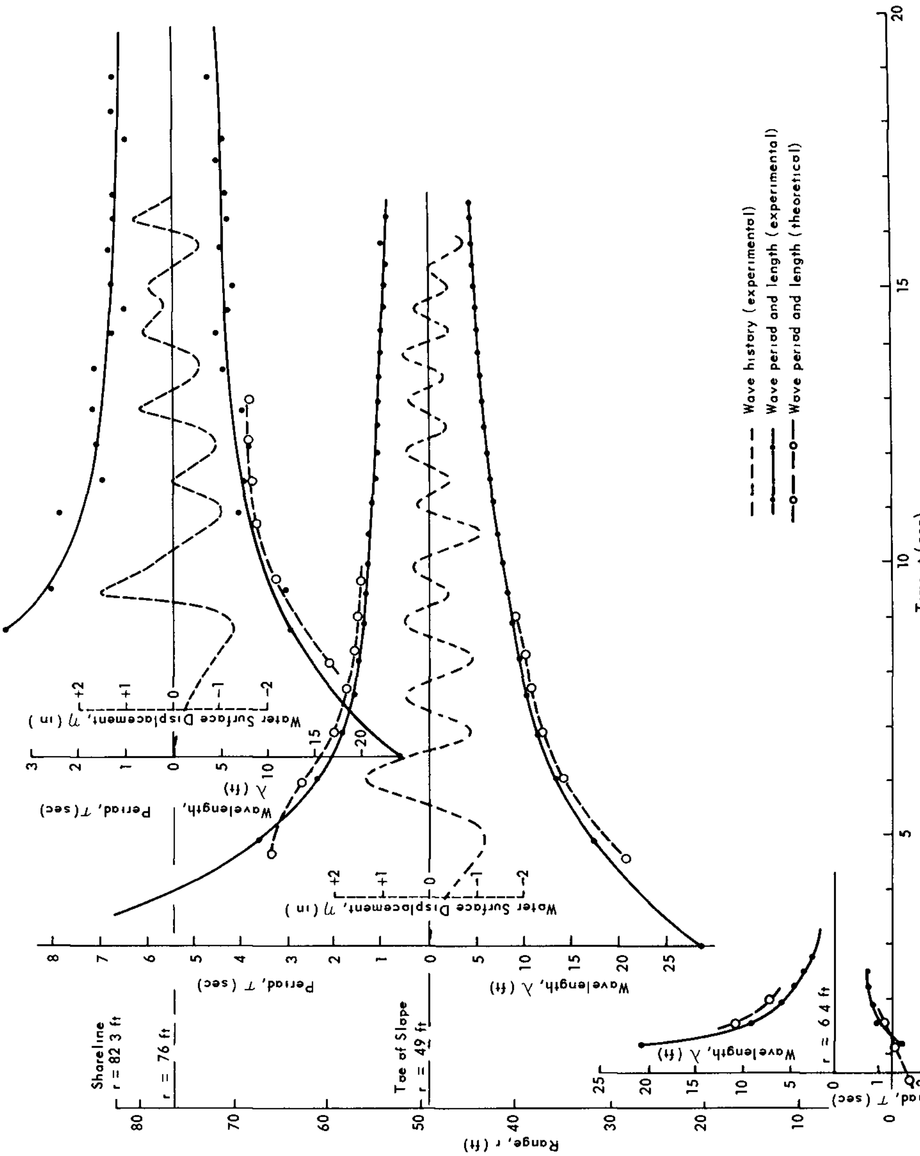

Figure 5. Comparison of time-variation of dispersive properties of theoretical and experimental waves, shallow-water case with crater size adjusted.

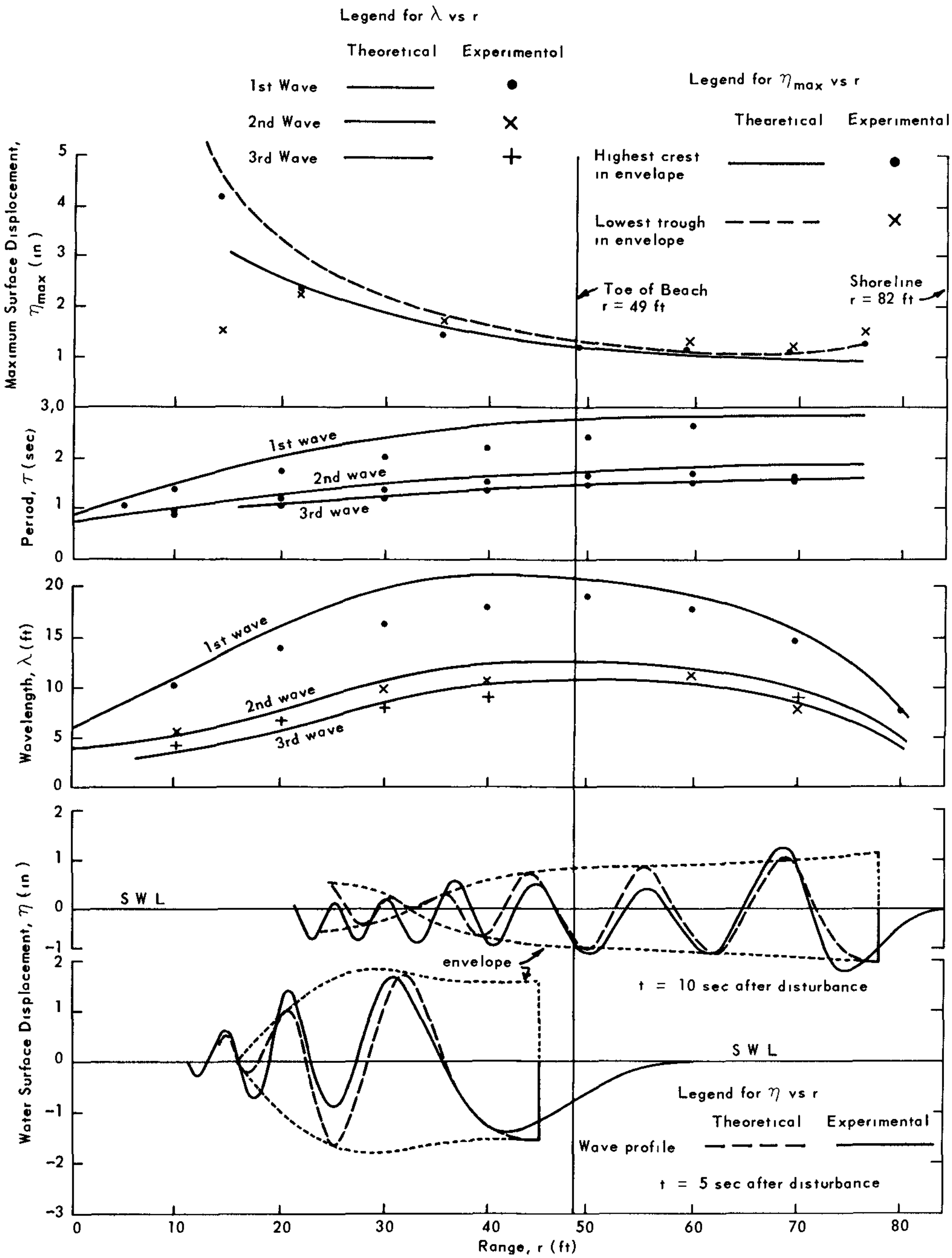

Figure 6 Comparison of space-variation of dispersive properties of theoretical and experimental waves, shallow-water case with crater size adjusted.

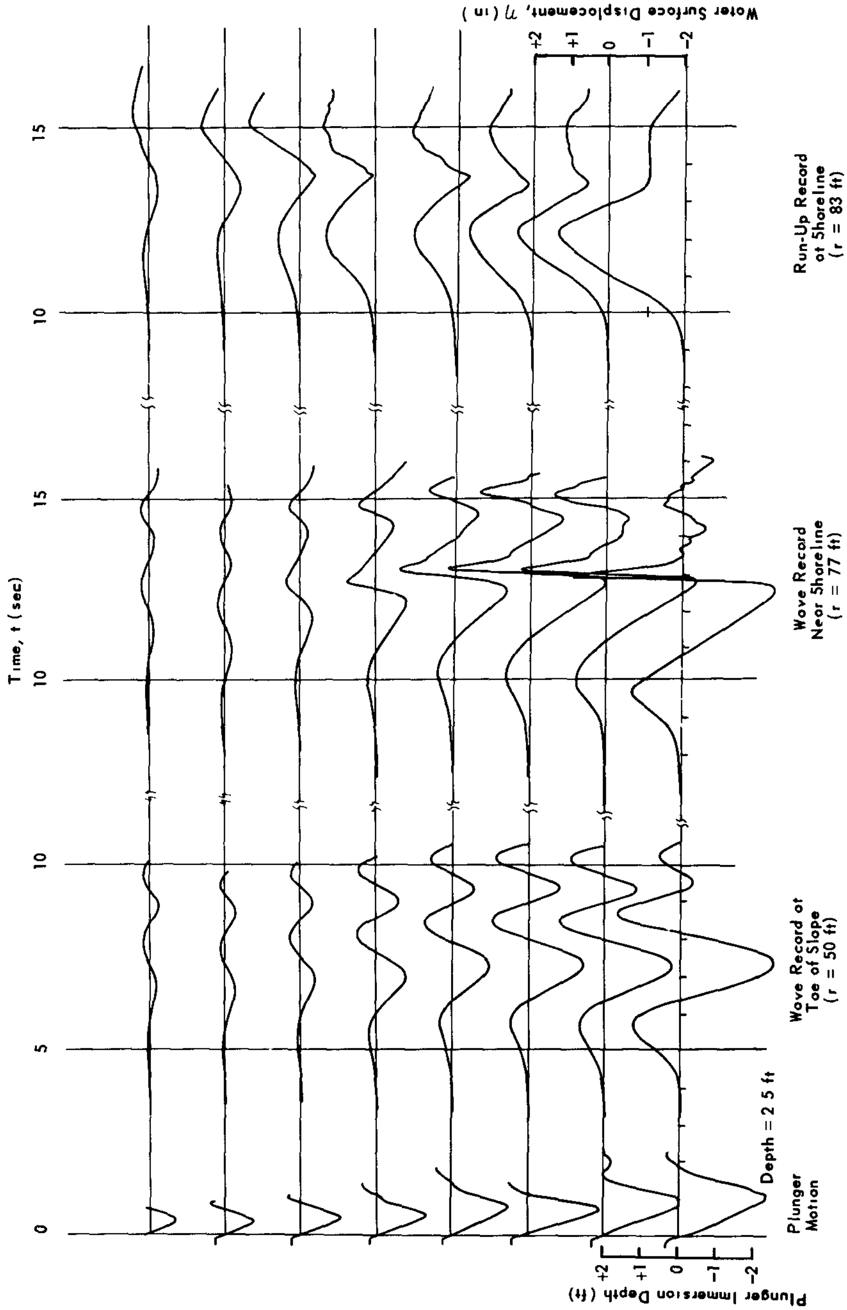

Figure 7. Effect of size of disturbance on wave form and run-up.

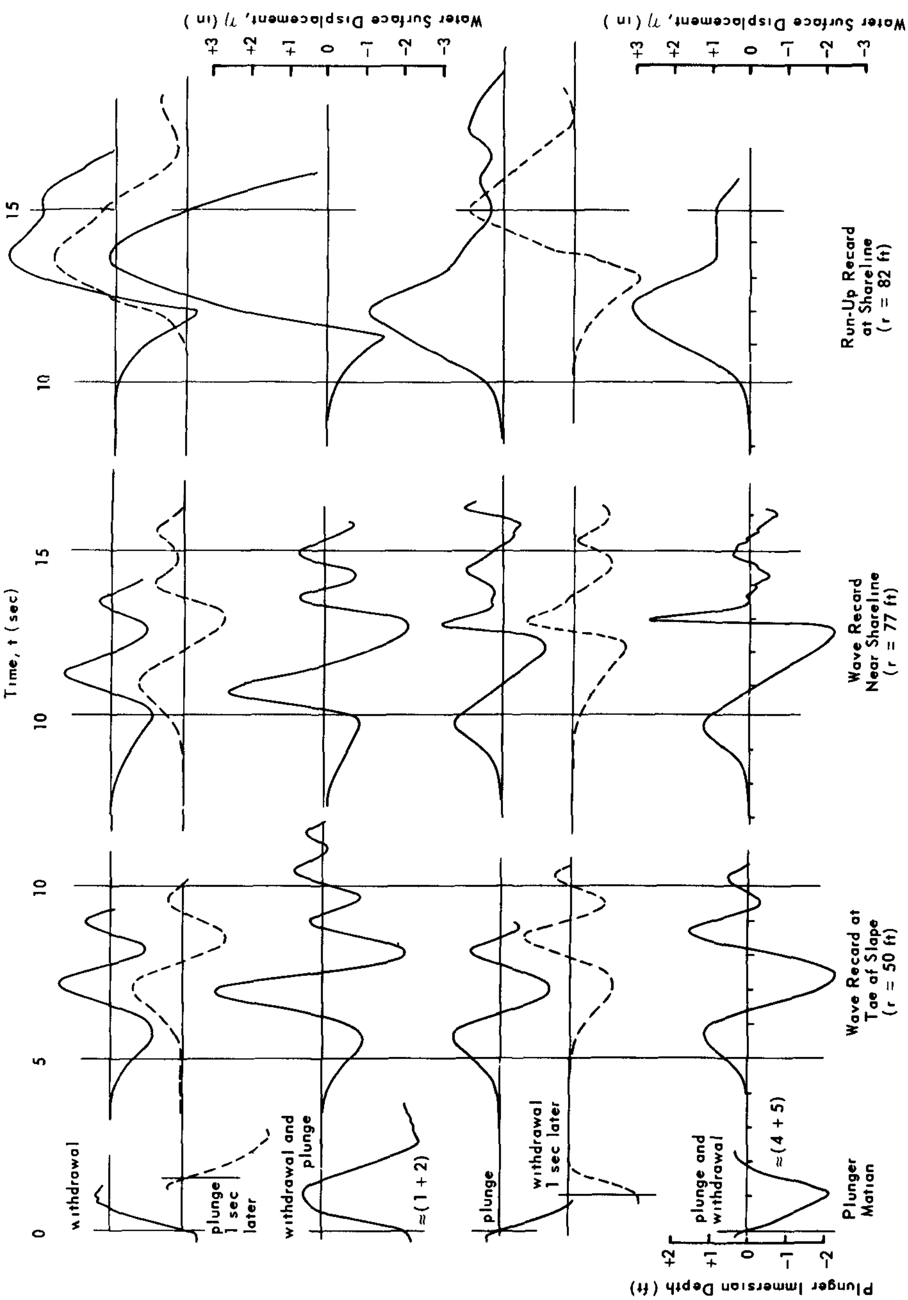

Figure 8. Effect of mode of disturbance on wave form and run-up.